126 GeV Higgs in next-to-minimal Universal Extra Dimensions ☆

Thomas Flacke [a], Kyoungchul Kong [b], Seong Chan Park [c],*

[a] *Department of Physics, Korea Advanced Institute of Science and Technology, 335 Gwahak-ro, Yuseong-gu, Daejeon 305-701, Republic of Korea*
[b] *Department of Physics and Astronomy, University of Kansas, Lawrence, KS 66045, USA*
[c] *Department of Physics, Sungkyunkwan University, Suwon 440-746, Republic of Korea*

A B S T R A C T

The discovery of a Higgs boson and precise measurements of its properties open a new window to test physics beyond the standard model. Models with Universal Extra Dimensions are not an exception. Kaluza–Klein excitations of the standard model particles contribute to the production and decay of the Higgs boson. In particular, parameters associated with third generation quarks are constrained by Higgs data, which are relatively insensitive to other searches often involving light quarks and leptons. We investigate implications of the 126 GeV Higgs in next-to-minimal Universal Extra Dimensions, and show that boundary terms and bulk masses allow a lower compactification scale as compared to in minimal Universal Extra Dimensions.

© 2013 The Authors. Published by Elsevier B.V. All rights reserved.

1. Introduction

The recent discovery of a Higgs-like boson at the LHC and measurements of its properties open a new window for physics beyond the Standard Model (SM). Both the ATLAS and the CMS Collaborations have measured its mass with precision better than that in the top quark mass (0.5%):

$$m_H = \begin{cases} 125.5 \pm 0.2^{+0.5}_{-0.6} \text{ GeV}, & \text{ATLAS (0.43\% precision) [1]}, \\ 125.7 \pm 0.3 \pm 0.3 \text{ GeV}, & \text{CMS (0.34\% precision) [2]}. \end{cases} \quad (1)$$

Measured properties of the boson are consistent with the standard model expectation, which is often parameterized by $\mu = \sigma/\sigma_{SM}$, the ratio between the SM expectation and the measured value:

$$\mu = \begin{cases} 1.30 \pm 0.20, & \text{ATLAS [1]}, \\ 0.80 \pm 0.14, & \text{CMS [2]}. \end{cases} \quad (2)$$

We regard that the discovered boson is actually the Higgs boson in the SM and try to set bounds on new physics models by comparing the measured data and the expected deviation from new physics. In general, the radiative production of the Higgs boson through gluon fusion and its decay to a pair of photons are subject to modification by heavy new colored particles, namely the 'top partner' (t') [3] and electrically charged particles, namely charged gauge bosons and heavy leptons (W' and ℓ'). Any new physics model which contains such new particles affects the Higgs physics and can be probed by close examination of the Higgs data.

In models with Universal Extra Dimensions (UED) [4], all the standard model particles have their Kaluza–Klein (KK) excitations, including new colored particles and electrically charged particles. Among them, the KK excitations of the top quark yield significant corrections to the gluon fusion process due to the largest Yukawa coupling. As the fermionic degrees of freedom in models with extra dimensions are doubled, the KK top quark contribution is also enhanced by a factor of 2. Also, both the KK W bosons and the KK top quarks contribute to the one-loop induced decay rate to the diphoton. Even though one-loop suppressed, the diphoton channel has been regarded as one of a golden channels. Other decay channels, which are allowed at tree level, are less significantly modified by the KK states so that we may neglect these effects here. There are existing studies on the Higgs production and decay rates in the minimal UED (MUED) model [5,6] as well as various 5D [7] and 6D extensions [8].

In this Letter, we extend the previous studies by including effects of bulk mass parameters [9–11] and boundary localized terms [12,13] following the philosophy of a recent paper [14]. In Ref. [14]

it was shown that bulk masses are strongly constrained for leptons and the first two quark families. Furthermore, non-uniform boundary terms and bulk masses for leptons, and first and second family quarks typically imply large flavor changing neutral currents and are thus strongly constrained [15]. As an important exception, a common boundary parameter for all UED fields is not constrained as it does not induce KK-number violating interactions and only shifts the overall mass scale of the nth Kaluza–Klein mode excitations away from n/R, with R being the compactification radius of the extra dimension.

Constraints on parameters associated with third generation quarks are much weaker, and their phenomenological implications are very different from those with first and second generations. They are particularly important in physics dominated by one-loop corrections, where the large Yukawa coupling of the top plays a crucial role. This applies to electroweak precision tests as well as to Higgs production and decay. We therefore focus on the third generation in the quark sector and consider a UED setup with a common boundary kinetic parameter r_g for the gauge and lepton sector and the first two families (and no bulk masses for those). We allow for a non-zero bulk mass ($\mu_t \neq 0$) and a different boundary parameter r_t for the third generation. This choice leaves us with r_g, r_t, μ_t and R^{-1} as parameters to be constrained.

The Letter is organized as follows. In the next section, we briefly introduce the next-to-minimal UED (NMUED) model with bulk mass parameters and boundary localized terms. The KK spectra and couplings are collected for the one-loop calculation of the gluon fusion process and radiative decay processes in Section 3 and the electroweak bounds are considered in Section 4. We show our results in Section 5 taking the latest experimental results into account.

2. Next-to-minimal Universal Extra Dimensions

The minimal UED action contains gauge invariant kinetic terms for the bulk fields and Yukawa interaction terms, assuming vanishing boundary localized terms at the cutoff scale. In NMUED, we introduce bulk mass and boundary terms for the third generation and a generic boundary term, which are parameterized as

$$S_{NMUED} = S_{MUED} + \int d^4 x \int_{-L}^{L} dy \left\{ -M_t \xi_{L/R} \overline{\Psi}_3 \Psi_3 \right.$$
$$+ \left[\delta(y - L) + \delta(y + L) \right]$$
$$\left. \times \left[r_g \mathcal{L}_{MUED} + (r_t - r_g) i \overline{\Psi}_{3,L/R} \slashed{D} \Psi_{3,L/R} \right] \right\}, \quad (3)$$

where $L = \pi R/2$ with R being the compactification radius, $\xi_{L/R} = \pm 1$, and $\Psi_3 = \{Q_3, T, B\}$ are 5D fermions containing the third generation quarks, of which Q_3 has a left-handed and T, B have right-handed boundary terms with a parameter r_t.[1] Both, bulk masses and boundary terms modify the masses and wave functions of the KK modes. A fermion Ψ with a left-handed zero mode (i.e. Q and L) in the presence of a boundary parameter r_t and a bulk mass $M_t = \mu_t \theta(y)$ is decomposed as follows.

$$\Psi(x, y) = \sum_{n=0}^{\infty} \left(\psi_L^{(n)}(x) f_n^{\Psi_L}(y) + \psi_R^{(n)}(x) f_n^{\Psi_R}(y) \right), \quad (4)$$

---

[1] The boundary localized terms are interpreted as operators generically allowed by symmetries of the system: 4D Lorentz symmetry on boundaries and gauge symmetries. The actual values of r_t and r_g could not be fully determined without knowing UV completion but we are only allowed to stay in the parameter space, which is consistent with the experimental results. Our choice of uniform terms is well consistent with the lack of flavor changing neutral current and also EWPTs for which the effects from the third generation are small.

where the wave functions $f_n^{\Psi_{L/R}}$ are given by

$$n = 0: \quad f_0^{\Psi_L} = N_0^\Psi e^{\mu_t |y|}, \quad (5)$$

$$\text{odd } n: \begin{cases} f_n^{\Psi_L} = N_n^\Psi \sin(k_n y), \\ f_n^{\Psi_R} = N_n^\Psi \left(-\dfrac{k_n}{m_{f_n}} \cos(k_n y) + \dfrac{\mu_t}{m_{f_n}} \theta(y) \sin(k_n y) \right), \end{cases}$$
$$(6)$$

$$\text{even } n: \begin{cases} f_n^{\Psi_L} = N_n^\Psi \left(\dfrac{k_n}{m_{f_n}} \cos(k_n y) + \dfrac{\mu_t}{m_{f_n}} \theta(y) \sin(k_n y) \right), \\ f_n^{\Psi_R} = N_n^\Psi \sin(k_n y). \end{cases}$$
$$(7)$$

where

$$\theta(y) = \begin{cases} -1 & \text{if } y < 0, \\ +1 & \text{if } y > 0, \end{cases}$$

as defined in Ref. [9]. The symbols $\sin$ and $\cos$ denote sin or sinh and cos or cosh, and wave numbers k_n are the solutions of the mass quantization condition

$$k_n \cos(k_n L) = \left(r_t (m_{f_n})^2 + \mu_t \right) \sin(k_n L) \quad \text{for odd } n,$$
$$r_t k_n \cos(k_n L) = -(1 + r_t \mu_t) \sin(k_n L) \quad \text{for even } n. \quad (8)$$

The chiral zero mode is massless. If "light" (sinh and cosh) solutions exist, they describe the first and second KK excitations, and their masses m_{f_n} are given by

$$m_{f_n} = \sqrt{-k_n^2 + \mu_t^2}, \quad (9)$$

while the "heavy" KK modes (sin and cos solutions) have masses

$$m_{f_n} = \sqrt{k_n^2 + \mu_t^2}. \quad (10)$$

The normalization factors are given by

$$N_n^\Psi = \begin{cases} \sqrt{\dfrac{\mu_t}{(1 + 2 r_t \mu_t) \exp(2\mu_t L) - 1}} & \text{for } n = 0, \\ \left(L - \dfrac{\cos(k_n L) \sin(k_n L)}{k_n} + 2 r_t \sin^2(k_n L) \right)^{-1/2} & \text{for odd } n, \\ \left(L - \dfrac{\cos(k_n L) \sin(k_n L)}{k_n} \right)^{-1/2} & \text{for even } n, \end{cases}$$
$$(11)$$

and they are determined from the modified orthogonality relations

$$\int_{-L}^{L} dy \, f_m^{\Psi_L} f_n^{\Psi_L} \left[1 + r_t \left[\delta(y + L) + \delta(y - L) \right] \right] = \delta_{mn},$$

$$\int_{-L}^{L} dy \, f_m^{\Psi_R} f_n^{\Psi_R} = \delta_{mn}. \quad (12)$$

A fermion with a right-handed zero mode (i.e. U, D, E) yields analogous results when replacing μ_t with $-\mu_t$.

The KK reduction of gauge bosons and scalars has been discussed in Ref. [16]. The fields are decomposed according to

$$A_\mu(x, y) = \sum_{n=0}^{\infty} A_\mu^{(n)}(x) f_n^A(y), \quad (13)$$

$$H(x, y) = \sum_{n=0}^{\infty} H^{(n)}(x) f_n^A(y). \quad (14)$$

For a uniform boundary kinetic term as considered in this article, the resulting wave functions are[2]

$$n = 0: \quad f_0^A(y) = \frac{1}{\sqrt{2L(1 + \frac{r_g}{L})}}, \tag{15}$$

$$\text{odd } n: \quad f_n^A(y) = \sqrt{\frac{1}{L + r_g \sin^2(k_n L)}} \sin(k_n y), \tag{16}$$

$$\text{even } n: \quad f_n^A(y) = \sqrt{\frac{1}{L + r_g \cos^2(k_n L)}} \cos(k_n y), \tag{17}$$

where the wave numbers k_n are determined by

$$\cot(k_n L) = r_g k_n \quad \text{for odd } n,$$
$$\tan(k_n L) = -r_g k_n \quad \text{for even } n, \tag{18}$$

and the corresponding KK masses are

$$m_{A_n} = \sqrt{k_n^2 + m_0^2}, \tag{19}$$

where m_0 is the zero mode mass (m_W, m_Z, m_H or zero), which is induced by electroweak symmetry breaking (EWSB). The wave functions satisfy the following orthogonality relation

$$\int_{-L}^{L} dy \, f_m^A f_n^A \big[1 + r_g\big(\delta(y+L) + \delta(y-L)\big)\big] = \delta_{mn}. \tag{20}$$

As expected, the masses and wave functions for scalars and gauge bosons are identical to those of the Z_2-even fermions in the limit $\mu_t \to 0$.

The couplings are obtained from overlap integrals of the respective wave functions. As an example, the coupling of a zero mode gauge boson with KK mode fermions follows from

$$S_{eff} \supset \int d^4x \, ig_5 \overline{\psi}_{L/R}^{(n)} \gamma^\mu A_\mu^{(0)} \psi_{L/R}^{(m)}$$
$$\times \int_{-L}^{L} dy \, f_0^A f_n^{\Psi_{L/R}} f_m^{\Psi_{L/R}} \big[1 + r_t\big(\delta(y+L) + \delta(y-L)\big)\big]$$
$$= \int d^4x \, i \frac{g_5 \delta_{nm}}{\sqrt{2L(1 + r/L)}} \overline{\psi}_{L/R}^{(n)} \gamma^\mu A_\mu^{(0)} \psi_{L/R}^{(m)}, \tag{21}$$

implying that

$$g_{0nm}^{eff} = \frac{g_5 \delta_{nm}}{\sqrt{2L(1 + r/L)}} = g_{SM} \delta_{nm}, \tag{22}$$

where g_{SM} is the standard model coupling. All couplings of zero mode gauge bosons to KK fermions are Kaluza–Klein number conserving and of strength g_{SM}, i.e. independent of the fermion KK level. Calculation of the analogous overlap integrals yields the same result for couplings of zero mode gauge bosons to KK gauge bosons, and of the zero mode Higgs to KK mode fermions or gauge bosons. Interactions between the zero mode Higgs and KK fermions are given by the standard model Yukawa couplings if we assume the same mass and boundary terms for Q_3, U_3, and D_3, which is the case in our current study.

---

[2] For generic choices of the boundary parameters, the KK decomposition in the electroweak sector is more involved. For a detailed discussion and the general solutions, we refer to Ref. [16].

3. Higgs production and decay into photons in NMUED

In the standard model, the production and decay processes of the Higgs boson, $gg \to H$ and $H \to \gamma\gamma$, are radiatively induced by triangle diagrams where top quark and W boson are involved. In NMUED, there are additional contributions from the Kaluza–Klein partners amongst which KK-top and KK W-loops dominate.

For a general triangle diagram, KK number is not necessarily conserved in the loop which in particular requires to sum over all allowed combinations of KK numbers in the loop when calculating the amplitude. For Higgs production and decay, however, all external lines are zero mode bosons (photon, gluon or Higgs), which preserve KK number as shown in the last section. Furthermore, as shown in Eq. (22), the 0–n–n couplings are all given by the corresponding standard model couplings. Therefore, the NMUED contributions to $gg \to H$ and $H \to \gamma\gamma$ can be easily calculated from the standard model expressions (cf. [17] and [6]) by replacing the standard model masses with the masses of the respective KK particles given in Eqs. (9), (10), (19) and summing over all KK modes. Note that the KK fermions are Dirac and therefore enter with twice the weight of the standard model fermions.

Through triangle diagrams with W-bosons, top quarks and their Kaluza–Klein excitations, the Higgs boson would decay to a pair of gluons and photons with the widths:

$$\Gamma_{H \to gg}^{NMUED} = \mathcal{K} \frac{m_H^3}{8\pi v^2} \cdot \frac{\alpha_S(m_H)^2}{\pi^2} |F_t|^2, \tag{23}$$

$$\Gamma_{H \to \gamma\gamma}^{NMUED} = \frac{m_H^3}{16 v^2 \pi} \cdot \frac{\alpha(m_H)^2}{\pi^2} \big|F_W + 3 Q_t^2 F_t\big|^2, \tag{24}$$

where $\mathcal{K} \approx 1.9$ is the QCD $\mathcal{K}$ factor in NNLO calculation [18], the Higgs vacuum expectation value is $v = (\sqrt{2} G_F)^{-1/2}$ with the Fermi constant $G_F = 1.1663787(6) \times 10^{-5}$ GeV^{-2} and $Q_t = 2/3$ is electric charge of the top quark. The one-loop functions are the sum of the SM contribution and the KK contributions: $F_W = F_W^{SM} + F_W^{KK}$, $F_t = F_t^{SM} + F_t^{KK}$ with

$$F_W^{SM} = \frac{1}{2} + \frac{3}{4}\tau_W + \frac{3}{2}\tau_W\left(1 - \frac{\tau_W}{2}\right)C_0(\tau_W),$$

$$F_W^{KK} = \sum_{n=1}^{\infty}\left[\frac{1}{2} + \tau_W + 2\left(\tau_W\left(1 - \frac{\tau_{W_n}}{2}\right) - \frac{\tau_{W_n}}{4}\right)C_0(\tau_{W_n})\right],$$

$$F_t^{SM} = -\frac{\tau_t}{2}\big[1 + (1 - \tau_t)C_0(\tau_t)\big],$$

$$F_t^{KK} = \sum_{n=1}^{\infty}\left[\frac{\tau_t}{\tau_{t_n^L}}F_t^{SM}(\tau_t \to \tau_{t_n^L}) + \frac{\tau_t}{\tau_{t_n^R}}F_t^{SM}(\tau_t \to \tau_{t_n^R})\right], \tag{25}$$

where the masses are conveniently parameterized as $\tau_W = 4m_W^2/m_H^2$, $\tau_t = 4m_t^2/m_H^2$, $\tau_{W_n} = 4m_{W_n}^2/m_H^2$ and $\tau_{t_n^{L/R}} = (4m_{t_n^{L/R}}^2)/(m_H^2)$. The three point Passarino–Veltman function is $C_0(\tau) = [\sin^{-1}(1/\sqrt{\tau})]^2$ for $\tau \geqslant 1$. F_W^{KK} includes contributions of KK excitations in the gauge and Higgs sectors. The production cross section $\hat{\sigma}_{gg \to H}(\hat{s})$ is related to the partial decay width as follows,

$$\hat{\sigma}_{gg \to H}(\hat{s}) = \frac{\pi^2}{8m_H} \Gamma_{H \to gg}(m_H) \delta(\hat{s} - m_H^2). \tag{26}$$

4. Electroweak precision tests (S, T, U) parameters

A strong bound on the NMUED model arises from contributions to the Peskin–Takeuchi parameters S, T, and U [19], which parameterize the oblique corrections to the electroweak gauge boson propagators [20]. The analysis of the Peskin–Takeuchi parameters
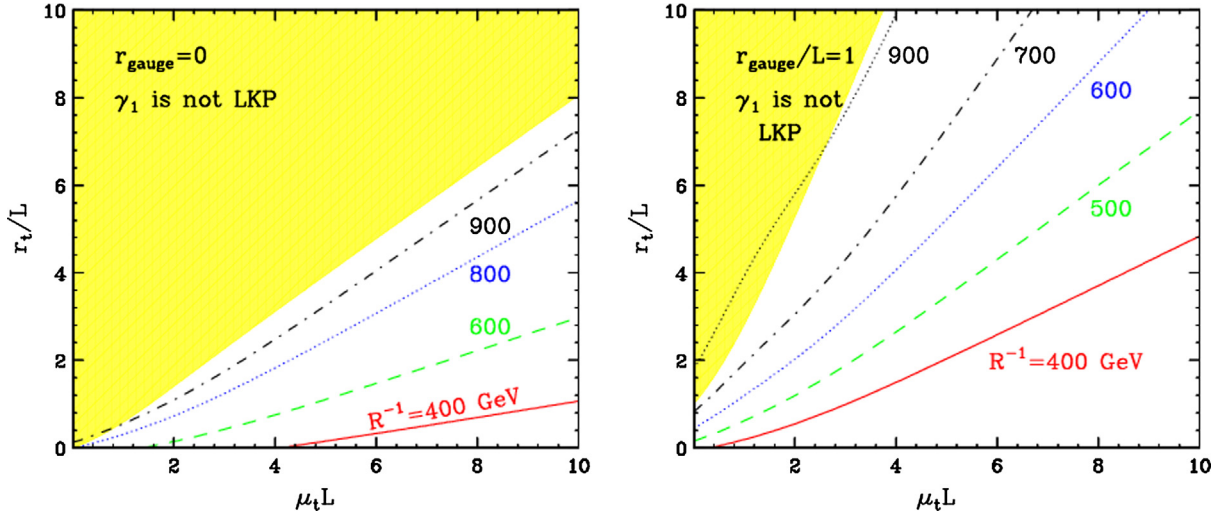
Fig. 1. Oblique (S, T, U) bounds on R^{-1} with the latest Gfitter data with $m_H = 126$ GeV. The plots show contours of minimally allowed R^{-1} in the r_t/L vs. $\mu_t L$ parameter space for $r_g/L = 0$ (left) and $r_g/L = 1$ (right). The shaded region (in yellow) is excluded since KK bottom is the lightest Kaluza–Klein particle. (For interpretation of the references to color in this figure legend, the reader is referred to the web version of this article.)

in UED models with bulk masses and boundary kinetic terms has been performed in Ref. [14]. The dominant contributions to S and T arise from the top-loop corrections to the gauge boson propagators, while U only receives contributions from gauge boson and Higgs loops. At one-loop order, the NMUED contributions to the Peskin–Takeuchi parameters are [14,19][3]

$$S_{NMUED} = \frac{4\sin^2\theta_W}{\alpha}\left[\frac{3g_{ew}^2}{4(4\pi)^2}\left(\frac{2}{9}\sum_n \frac{m_t^2}{m_{t^{(n)}}^2}\right)\right.$$
$$\left.+ \frac{g_{ew}^2}{4(4\pi)^2}\left(\frac{1}{6}\sum_n \frac{m_h^2}{m_{h^{(n)}}^2}\right)\right], \tag{27}$$

$$T_{NMUED} = \frac{1}{\alpha}\left[\frac{3g_{ew}^2}{2(4\pi)^2}\frac{m_t^2}{m_W^2}\left(\frac{2}{3}\sum_n \frac{m_t^2}{m_{t^{(n)}}^2}\right)\right.$$
$$\left.+ \frac{g_{ew}^2 \sin^2\theta_W}{(4\pi)^2 \cos^2\theta_W}\left(-\frac{5}{12}\sum_n \frac{m_h^2}{m_{h^{(n)}}^2}\right)\right], \tag{28}$$

$$U_{NMUED} = -\frac{4\sin^2\theta_W}{\alpha}\left[\frac{g_{ew}^2 \sin^2\theta_W}{(4\pi)^2}\right.$$
$$\left.\times\left(\frac{1}{6}\sum_n \frac{m_W^2}{m_{W^{(n)}}^2} - \frac{1}{15}\sum_n \frac{m_W^2 m_h^2}{m_{W^{(n)}}^2 m_{h^{(n)}}^2}\right)\right]. \tag{29}$$

Here α is the fine structure constant, θ_W is the Weinberg angle, and g_{ew} is the coupling strength of $SU(2)_W$.

5. Results

In our analysis, for simplicity we consider a common bulk mass $\mu_t \equiv \mu_{Q_3} = \mu_B = \mu_T$ and a common boundary parameter $r_t \equiv r_{Q_3} = r_B = r_T$, for the third generation of $SU(2)_W$ quark doublet Q_3 and $SU(2)_W$ singlets B and T. This choice, together with the compactification scale R^{-1}, leaves us with three parameters. As an additional parameter, we consider a common boundary parameter r_g for all other fields (i.e. the Higgs, the gauge fields and

leptons, and the first and second family quarks) in order to illustrate how the bounds change in the presence of a common boundary parameter with only the third family quarks differing. We present results as bounds on the compactification scale R^{-1} as a function of the dimensionless parameters $\mu_t L$ and r_t/L. To indicate the effect of a common boundary term, we show constraints for $r_g/L = 0$ ("vanishing boundary parameter") and $r_g/L = 1$ ("typical boundary parameter").[4]

The electroweak bounds shown in Fig. 1 are obtained by performing a χ^2 fit of the parameters S_{NMUED}, T_{NMUED}, U_{NMUED} from Eqs. (27)–(29) to the experimental values given in Ref. [21], $S_{NP} = 0.03 \pm 0.10$, $T_{NP} = 0.05 \pm 0.12$, $U_{NP} = 0.03 \pm 0.10$, for a reference point $m_H = 126$ GeV and $m_t = 173$ GeV with correlation coefficients of $+0.89$ between S_{NP} and T_{NP}, and -0.54 (-0.83) between S_{NP} and U_{NP} (T_{NP} and U_{NP}).

For $r_g/L = 0$, the mass of the first $U(1)_Y$ KK mode $\gamma^{(1)}$ (the usual UED dark matter candidate) is given by R^{-1}. For a large r_t/L and a small μ_t/L, the first KK bottom partner is lighter than the $\gamma^{(1)}$ which implies a charged dark matter and is therefore excluded. For $r_g/L \neq 0$, the same applies, although the mass of the $\gamma^{(1)}$ is not given by R^{-1} anymore, but determined by Eq. (18).

To determine the bounds from Higgs searches, we define the signal strengths as follows:

$$\mu_{gg\to h\to\gamma\gamma} \equiv \frac{\hat{\sigma}_{gg\to h\to\gamma\gamma}^{NMUED}}{\hat{\sigma}_{gg\to h\to\gamma\gamma}^{SM}} = \frac{|F_t|^2|F_W + 3Q_t^2 F_t|^2}{|F_t^{SM}|^2|F_W^{SM} + 3Q_t^2 F_t^{SM}|^2}, \tag{30}$$

$$\mu_{other\to h\to\gamma\gamma} \equiv \frac{\hat{\sigma}_{other\to h\to\gamma\gamma}^{NMUED}}{\hat{\sigma}_{other\to h\to\gamma\gamma}^{SM}} = \frac{|F_W + 3Q_t^2 F_t|^2}{|F_W^{SM} + 3Q_t^2 F_t^{SM}|^2}, \tag{31}$$

$$\mu_{gg\to h\to other} \equiv \frac{\hat{\sigma}_{gg\to h\to other}^{NMUED}}{\hat{\sigma}_{gg\to h\to other}^{SM}} = \frac{|F_t|^2}{|F_t^{SM}|^2}, \tag{32}$$

$$\mu_{other\to h\to other} \equiv \frac{\hat{\sigma}_{other\to h\to other}^{NMUED}}{\hat{\sigma}_{other\to h\to other}^{SM}} = 1, \tag{33}$$

where "other" production channels are vector boson fusion, and Higgs radiation off gauge bosons or tops, and "other" decay chan-

---

[3] In Ref. [14], additional contributions to T and U arise due to lepton bulk mass terms, which are however shown to be strongly constraint by dilepton searches. Here, we assume vanishing lepton bulk masses and therefore neglect such contributions.

[4] A naive dimensional analysis of the boundary parameter yields $r/L \lesssim 12/\Lambda R$, where Λ is the UED cutoff scale, and ΛR gives an estimate for the number of KK levels below the cutoff scale [12].
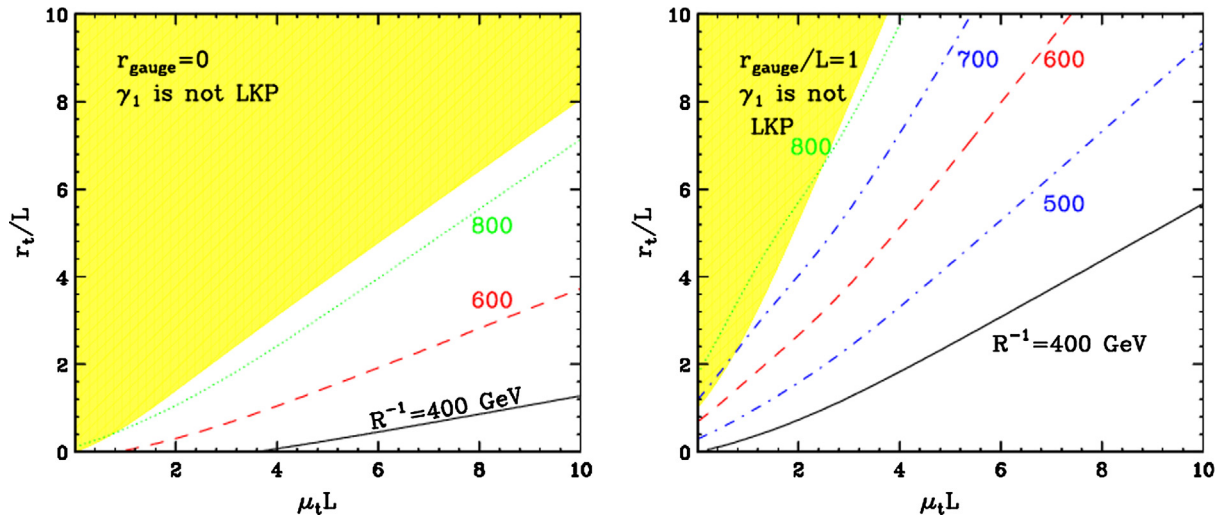
Fig. 2. Combined constraints from Higgs searches at ATLAS and CMS. The plots show contours of minimally allowed R^{-1} in the r_t/L vs. μ_t/L parameter space for $r_g/L = 0$ (left) and $r_g/L = 1$ (right). The shaded region (in yellow) is excluded since the Kaluza–Klein photon is not a dark matter candidate. (For interpretation of the references to color in this figure legend, the reader is referred to the web version of this article.)

nels are ZZ, WW, $b\bar{b}$, and $\tau\tau$. Ref. [22] performs a global Bayesian analysis on the ATLAS [23] and CMS [24] Higgs data and provides values of signal strengths and their correlations. We use this data to perform a χ^2 test of the UED predictions and plot the constraints in Fig. 2 where no correlation between the ATLAS and CMS results is assumed.

Compared to the electroweak constraints and the CMS bounds, the ATLAS bounds are weaker. The main reason for this lies in that ATLAS (CMS) observes an enhanced (reduced) rate in the di-photon channel as compared to the standard model expectation. The UED model predicts an enhancement of the cross section for $gg \rightarrow h \rightarrow \gamma\gamma$.[5] The other channels do not have a strong effect on the χ^2 fit because of the larger errors. Therefore, the constraints shown in Fig. 2 are dominated by the measurements at CMS. We note that the bound from electroweak precision tests is comparable with the bound from direct Higgs searches.

6. Summary and outlook

UED is an attractive extension of the standard model based on higher dimensions providing a viable dark matter candidate and rich phenomenology at the LHC. As an effective theory, UED models could be extended from the minimal realization by incorporating boundary localized operators and bulk masses. In this Letter, we focus on the extra terms associated with the third generation of quarks, which are particularly relevant for the radiative production and decay of the Higgs boson through the Kaluza–Klein quarks and W-bosons. Including electroweak precision tests as well as the latest measurements on the Higgs boson at the LHC (ATLAS and CMS), we explicitly show the allowed range of parameter space in next-to-minimal UED for the Kaluza–Klein photon dark matter candidate. Our results show that NMUED allows for a lower compactification scale than as in MUED, where $R^{-1} < 500$ GeV is

excluded at 95% C.L. [6].[6] This allowed parameter space will be probed by the LHC14.

References

[1] ATLAS Collaboration, Combined measurements of the mass and signal strength of the Higgs-like boson with the ATLAS detector using up to 25 fb^{-1} of proton–proton collision data, ATLAS-CONF-2013-014.
[2] CMS Collaboration, Combination of standard model Higgs boson searches and measurements of the properties of the new boson with a mass near 125 GeV, CMS-PAS-HIG-13-005.
[3] K. Kong, S.C. Park, Phenomenology of top partners at the ILC, J. High Energy Phys. 0708 (2007) 038, arXiv:hep-ph/0703057.
[4] T. Appelquist, H.C. Cheng, B.A. Dobrescu, Bounds on universal extra dimensions, Phys. Rev. D 64 (2001) 035002, arXiv:hep-ph/0012100.
[5] F.J. Petriello, Kaluza–Klein effects on Higgs physics in universal extra dimensions, J. High Energy Phys. 0205 (2002) 003, arXiv:hep-ph/0204067.
[6] G. Belanger, A. Belyaev, M. Brown, M. Kakizaki, A. Pukhov, Testing minimal universal extra dimensions using Higgs boson searches at the LHC, Phys. Rev. D 87 (2013) 016008, arXiv:1207.0798 [hep-ph].
[7] U.K. Dey, T.S. Ray, Constraining minimal and non-minimal UED models with Higgs couplings, Phys. Rev. D 88 (2013) 056016, arXiv:1305.1016 [hep-ph].
[8] T. Kakuda, K. Nishiwaki, K.-y. Oda, R. Watanabe, Universal extra dimensions after Higgs discovery, Phys. Rev. D 88 (2013) 035007, arXiv:1305.1686 [hep-ph].
[9] S.C. Park, J. Shu, Split universal extra dimensions and Dark Matter, Phys. Rev. D 79 (2009) 091702, arXiv:0901.0720 [hep-ph].
[10] G.-Y. Huang, K. Kong, S.C. Park, Bounds on the fermion-bulk masses in models with universal extra dimensions, J. High Energy Phys. 1206 (2012) 099, arXiv:1204.0522 [hep-ph].

---

[5] To be more precise, the decay rate $h \rightarrow \gamma\gamma$ is reduced due to negative interference of the KK top and KK W loop contributions with the standard model contribution, but the production cross section $gg \rightarrow h$ is enhanced and leads to an enhancement of the overall cross section. The UED cross sections for $gg \rightarrow h \rightarrow other$ are enhanced even more, which again is partially reflected in some search channels at ATLAS, but not at CMS.

[6] The analysis in Ref. [6] is based on earlier ATLAS and CMS Higgs data. With the data set used here, these bounds are expected to increase. In the $0 = \mu_t = r_t = r_g$ limit of our analysis, we find $R^{-1} \lesssim 700$ GeV excluded. To our knowledge, the currently strongest published MUED bound from other collider searches is $R^{-1} < 715$ GeV [25].

[11] K. Kong, S.C. Park, T.G. Rizzo, Collider phenomenology with split-UED, J. High Energy Phys. 1004 (2010) 081, arXiv:1002.0602 [hep-ph].

[12] M.S. Carena, T.M.P. Tait, C.E.M. Wagner, Branes and orbifolds are opaque, Acta Phys. Pol. B 33 (2002) 2355, arXiv:hep-ph/0207056.

[13] G.R. Dvali, G. Gabadadze, M. Kolanovic, F. Nitti, The power of brane-induced gravity, Phys. Rev. D 64 (2001) 084004, arXiv:hep-ph/0102216;
F. del Aguila, M. Perez-Victoria, J. Santiago, Effective description of brane terms in extra dimensions, J. High Energy Phys. 0610 (2006) 056, arXiv:hep-ph/0601222.

[14] T. Flacke, K. Kong, S.C. Park, Phenomenology of universal extra dimensions with bulk-masses and brane-localized terms, J. High Energy Phys. 1305 (2013) 111, arXiv:1303.0872 [hep-ph].

[15] C. Csaki, J. Heinonen, J. Hubisz, S.C. Park, J. Shu, 5D UED: flat and flavorless, J. High Energy Phys. 1101 (2011) 089, arXiv:1007.0025 [hep-ph].

[16] T. Flacke, A. Menon, D.J. Phalen, Non-minimal universal extra dimensions, Phys. Rev. D 79 (2009) 056009, arXiv:0811.1598 [hep-ph].

[17] J.F. Gunion, H.E. Haber, G.L. Kane, S. Dawson, The Higgs hunter's guide, Front. Phys. 80 (2000) 1.

[18] V. Ravindran, J. Smith, W.L. van Neerven, NNLO corrections to the total cross-section for Higgs boson production in hadron hadron collisions, Nucl. Phys. B 665 (2003) 325, arXiv:hep-ph/0302135.

[19] T. Appelquist, H.U. Yee, Universal extra dimensions and the Higgs boson mass, Phys. Rev. D 67 (2003) 055002, arXiv:hep-ph/0211023;
I. Gogoladze, C. Macesanu, Precision electroweak constraints on universal extra dimensions revisited, Phys. Rev. D 74 (2006) 093012, arXiv:hep-ph/0605207;
M. Baak, M. Goebel, J. Haller, A. Hoecker, D. Ludwig, K. Moenig, M. Schott, J. Stelzer, Updated status of the global electroweak fit and constraints on new physics, Eur. Phys. J. C 72 (2012) 2003, arXiv:1107.0975 [hep-ph].

[20] M.E. Peskin, T. Takeuchi, A new constraint on a strongly interacting Higgs sector, Phys. Rev. Lett. 65 (1990) 964.

[21] M. Baak, M. Goebel, J. Haller, A. Hoecker, D. Kennedy, R. Kogler, K. Moenig, M. Schott, et al., The electroweak fit of the Standard Model after the discovery of a new boson at the LHC, arXiv:1209.2716 [hep-ph].

[22] B. Dumont, S. Fichet, G. von Gersdorff, A Bayesian view of the Higgs sector with higher dimensional operators, J. High Energy Phys. 1307 (2013) 065.

[23] ATLAS Collaboration, Measurements of the properties of the Higgs-like boson in the two photon decay channel with the ATLAS detector using 25 fb^{-1} of proton–proton collision data, ATLAS-CONF-2013-012;
ATLAS Collaboration, Combined measurements of the mass and signal strength of the Higgs-like boson with the ATLAS detector using up to 25 fb^{-1} of proton–proton collision data, ATLAS-CONF-2013-014;
ATLAS Collaboration, Measurements of the properties of the Higgs-like boson in the four lepton decay channel with the ATLAS detector using 25 fb^{-1} of proton–proton collision data, ATLAS-CONF-2013-013;
ATLAS Collaboration, Measurements of the properties of the Higgs-like boson in the $WW^{(*)} \rightarrow \ell\nu\ell\nu$ decay channel with the ATLAS detector using 25 fb^{-1} of proton–proton collision data, ATLAS-CONF-2013-030;
ATLAS Collaboration, Combined coupling measurements of the Higgs-like boson with the ATLAS detector using up to 25 fb^{-1} of proton–proton collision data, ATLAS-CONF-2013-034;
ATLAS Collaboration, Search for the Standard Model Higgs boson in produced in association with a vector boson and decaying to bottom quarks with the ATLAS detector, ATLAS-CONF-2012-161.

[24] CMS Collaboration, Updated measurements of the Higgs boson at 125 GeV in the two photon decay channel, CMS-PAS-HIG-13-001;
CMS Collaboration, Properties of the Higgs-like boson in the decay $H \rightarrow ZZ \rightarrow 4\ell$ in pp collisions at $\sqrt{s} = 7$ and 8 TeV, CMS-PAS-HIG-13-002;
CMS Collaboration, Evidence for a particle decaying to W^+W^- in the fully leptonic final state in a standard model Higgs boson search in pp collisions at the LHC, CMS-PAS-HIG-13-003;
CMS Collaboration, Search for SM Higgs in $WH \rightarrow WWW \rightarrow 3\ell3\nu$, CMS-PAS-HIG-12-039;
CMS Collaboration, Evidence for a particle decaying to W^+W^- in the fully leptonic final state in a standard model Higgs boson search in pp collisions at the LHC, CMS-PAS-HIG-12-042;
CMS Collaboration, Combination of standard model Higgs boson searches and measurements of the properties of the new boson with a mass near 125 GeV, CMS-PAS-HIG-12-045;
CMS Collaboration, Search for the standard model Higgs boson produced in association with W or Z bosons, and decaying to bottom quarks for HCP 2012, CMS-PAS-HIG-12-044;
CMS Collaboration, Search for Higgs boson production in association with top quark pairs in pp collisions, CMS-PAS-HIG-12-025;
CMS Collaboration, Search for the Standard-Model Higgs boson decaying to tau pairs in proton–proton collisions at $\sqrt{s} = 7$ and 8 TeV, CMS-PAS-HIG-13-004;
CMS Collaboration, Search for the standard model Higgs boson in the Z boson plus a photon channel in pp collisions at $\sqrt{s} = 7$ and 8 TeV, CMS-PAS-HIG-13-006;
CMS Collaboration, Combination of standard model Higgs boson searches and measurements of the properties of the new boson with a mass near 125 GeV, CMS-PAS-HIG-13-005.

[25] L. Edelhäuser, T. Flacke, M. Krämer, Constraints on models with universal extra dimensions from dilepton searches at the LHC, J. High Energy Phys. 1308 (2013) 091, arXiv:1302.6076 [hep-ph].